

Modeling Lightning Return Strokes to Tall Structures: A Review

Farhad Rachidi

Swiss Federal Institute of Technology (EPFL), EMC Group, CH-1015 Lausanne, Switzerland.

Abstract

In this paper, an overview of theoretical models of lightning return strokes to tall structures is presented. Simulation results are presented for the spatial and temporal distribution of the current along the channel and along the strike object, as well as for the electric and magnetic fields at different distances, making reference to available experimental data.

Index Terms

Lightning, Return Stroke, Tall Structures, Modeling, Engineering Models, Antenna-Theory Models, Electromagnetic Fields

1 INTRODUCTION

The interaction of lightning with tall strike-objects has recently attracted considerable attention of lightning researchers (e.g. [1]). Some of the return stroke models, initially developed for the case of return strokes initiated at ground, were extended to take into account the presence of a vertically-extended strike object. The presence of an elevated strike object have been included in two types -or classes- of return stroke models, namely the engineering models and the electromagnetic or Antenna-Theory (AT) models, as defined by Rakov and Uman [2]. In the engineering return stroke models, the spatial and temporal distribution of the channel current is specified based on observed characteristics such as channel-base current, return stroke speed and remote electromagnetic fields. The presence of an elevated strike object in such models have been considered by assuming the object as a uniform, lossless transmission line (e.g. [3]). In Antenna-Theory-type models (e.g. [4-7]) known as AT models, the strike object and the lightning channel are represented using thin wires. The Maxwell's equations are numerically solved using the method of moments [8] to find the current distribution along the lightning channel, from which the radiated electromagnetic fields can be computed. Hybrid-type models based on electromagnetic and circuit theory approaches have also been used by Visacro and co-workers (e.g. [9, 10]).

2 ENGINEERING MODELS

To analyze the interaction of lightning with tall strike objects, some of the engineering return stroke models, initially developed for the case of return strokes initiated at ground, were extended to take into account the presence of a vertically-extended strike object e.g., [11-25]. In some of these models, it is assumed that a current pulse $i_o(t)$ associated with the return-stroke process is injected at the lightning attachment point both into the strike object and into the lightning channel, e.g., [12, 13, 16-22, 26]. The upward-moving wave propagates along the channel at the return-stroke speed v as specified by the return-stroke model. The downward-moving wave propagates at the speed of light along the strike object, assumed to be a lossless uniform transmission line characterized by constant non-zero reflection coefficients at its top and its bottom. As noted in [14], the assumption of two identical current waves injected into the lightning channel and into the strike object implies that their characteristic impedances are equal to each other. This assumption makes the models not self-consistent in that (1) there is no impedance discontinuity at the tower top at the time of lightning attachment to the tower, but (2) there is one when the reflections from ground arrive at the tower top.

2.1 Extension of engineering models based on a distributed-source representation

Rachidi et al. [3] presented an extension of the so-called engineering return stroke models, taking into account the presence of a vertically-extended strike object, which does not employ the assumption that identical current pulses are launched both upward and downward from the object top. The extension is based on a distributed-source representation of the return-stroke channel [27, 28], which allows more general and straightforward formulations of these models than the traditional representations implying a lumped current source at the bottom of the channel.

The general equations for the spatial-temporal distribution of the current along the lightning channel and along the strike object have been derived [3]:

$$i(z', t) = \left[P(z'-h) i_o \left(h, t - \frac{z'-h}{v^*} \right) - \rho_t i_o \left(h, t - \frac{z'-h}{c} \right) + \right. \\ \left. + (1-\rho_t)(1+\rho_t) \sum_{n=0}^{\infty} \rho_t^{n+1} \rho_g^n i_o \left(h, t - \frac{h+z'}{c} - \frac{2nh}{c} \right) \right] u \left(t - \frac{z'-h}{v} \right) \\ \text{for } h < z' < H_0 \quad (1)$$

$$i(z', t) = (1-\rho_t) \sum_{n=0}^{\infty} \left[\rho_t^n \rho_g^n i_o \left(h, t - \frac{h-z'}{c} - \frac{2nh}{c} \right) + \right. \\ \left. + \rho_t^n \rho_g^{n+1} i_o \left(h, t - \frac{h+z'}{c} - \frac{2nh}{c} \right) \right] u \left(t - \frac{h+z'}{c} - \frac{2nh}{c} \right) \\ \text{for } 0 \leq z' \leq h \quad (2)$$

In (1) and (2),

- h is the height of the tower,
- ρ_t and ρ_g are the top and bottom current reflection coefficients for upward and downward propagating waves, respectively, given by

$$\rho_t = \frac{Z_t - Z_{ch}}{Z_t + Z_{ch}} \quad (3)$$

$$\rho_g = \frac{Z_t - Z_g}{Z_t + Z_g} \quad (4)$$

- H_0 is the height of the extending return stroke channel,
- c is the speed of light,
- $P(z')$ is a model-dependent attenuation function,
- $u(t)$ the Heaviside unit-step function,
- v is the return-stroke front speed, and
- v^* is the current-wave speed.

Expressions for $P(z')$ and v^* for some of the most commonly used return-stroke models are summarized in Table 1, in which λ is the attenuation height for the MTLE model and H_{tot} is the total height of the lightning channel.

Equations (1) and (2) are based on the concept of ‘undisturbed current’ $i_o(t)$, which represents the ‘ideal’ current that would be measured at the tower top if the current reflection coefficients at its both extremities were equal to zero.

It is assumed that the current reflection coefficients ρ_t and ρ_g are constant. In addition, any upward connecting leader and any reflections at the return stroke wavefront [20] are disregarded.

TABLE 1 - $P(z')$ AND v^* FOR DIFFERENT RETURN-STROKE MODELS (ADAPTED FROM [2]).

Model	$P(z')$	v^*
BG	1	∞
TCS	1	$-c$
TL	1	v
MTLL	$1 - z'/H_{tot}$	v
MTLE	$\exp(-z'/\lambda)$	v

2.2 Extension of engineering models based on a lumped series voltage source

Baba and Rakov [25, 29] proposed an alternative approach to Rachidi et al.’s distributed source representation [3], using a lumped series voltage source at the junction point between the channel and the strike object. They showed that such a representation assures appropriate boundary conditions at the attachment point and is equivalent to the distributed source representation [29]. In their representation, Baba and Rakov expressed the spatial-temporal distribution of the current along the strike object and along the channel in terms of the short-circuit current $i_{sc}(t)$, which is related to the undisturbed current through

$$i_{sc}(t) = 2i_o(t) \quad (5)$$

Furthermore, in [29], Baba and Rakov considered in their expressions a different speed v_{ref} for the upward propagating current waves reflected from the ground and then transmitted into the lightning channel.

2.3 On the representation of the elevated strike object

In all engineering models, the elevated strike object is modeled as an ideal transmission line. To include the structural nonuniformities of the elevated strike object, several transmission line sections in cascade have also been considered (e.g. [15, 30]). The transmission line representation of the elevated strike object has been shown to yield reasonable results in comparison with

experimental data. However, one should bear in mind that experimental data associated with lightning to tall structures are ‘affected’ by other, less-easily controlled factors such as the variability of lightning channel impedance and possible reflections at the return stroke wavefront [31]. In [32], Bermudez et al. presented an experimental validation of the transmission line representation of an elevated object struck by lightning. The experimental results were obtained using a reduced-scale model and injected signals with narrow pulse widths (down to 500 ps). The validation is performed using a reduced scale structure representing the Toronto CN Tower in Canada. Two models consisting, respectively, of 1-section and 3-section uniform transmission lines were considered for the comparison. It was shown that the 3 section model is able to accurately reproduce the obtained experimental data. The overall agreement between the 1-section model and the experimental results was also satisfactory, at least for the early-time response.

More recently, FDTD simulations performed by Baba and Rakov [33] suggest that the waveguide properties of a biconical antenna (representing a tower) depend on the direction of propagation. Precisely, while the current pulses suffer no attenuation while traveling from the tower apex to its base, the attenuation is significant when pulses propagate from the base to the apex [33]. This finding might render questionable the validity of reflection coefficients at ground level inferred from the measurements of current at the top of the tower.

2.4 Current distribution along the channel as predicted by engineering models

Pavanello et al. [34] compared the spatial-temporal distribution of the current predicted by engineering models, employing an undisturbed current $i_o(t)$, given by

$$i_o(h,t) = \frac{I_{o1}}{\eta} \frac{(t/\tau_1)^2}{1+(t/\tau_1)^2} e^{(-t/\tau_2)} + I_{o2} \left(e^{-t/\tau_3} - e^{-t/\tau_4} \right) \quad (6)$$

This undisturbed current is shown in Fig. 1, where the values of the parameters chosen are: $I_{o1} = 9.9$ kA, $\eta = 0.845$, $\tau_1 = 0.072$ μ s, $\tau_2 = 5.0$ μ s, $I_{o2} = 7.5$ kA, $\tau_3 = 100.0$ μ s, $\tau_4 = 6.0$ μ s. These values correspond to the channel-base current adopted in [35] to compare ground-initiated lightning return stroke models. Starting from the same undisturbed current, the spatial-temporal distribution of the current along the channel and along the strike object were calculated for each model.

In the calculation, the elevated strike object was assumed to have a height $h=168$ m, corresponding to the Peissenberg tower in Germany, and reflection coefficients are set respectively to $\rho_t = -0.53$ and $\rho_g = 0.7$ [36].

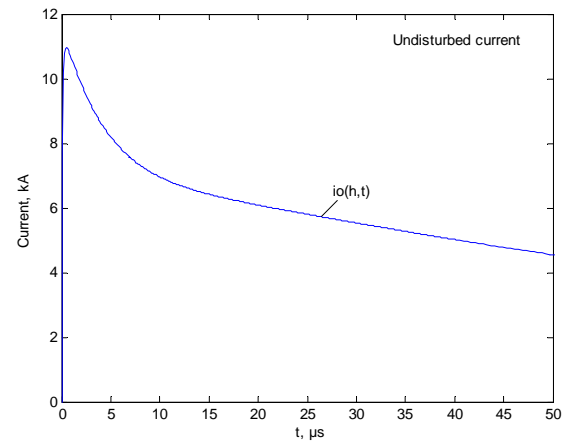


Fig. 1 - Undisturbed current (Adapted from[34])

Figures 2a-e show the current distribution along the tower and along the channel, at different time instants ($t=1, 2, \dots, 10$ μ s), predicted by each model. It can be seen that [34]

- in accordance with (2), the current distribution along the tower is independent of the model;
- the BG and TCS models exhibit a strong discontinuity at the return stroke wavefront, inherent in these models [2];

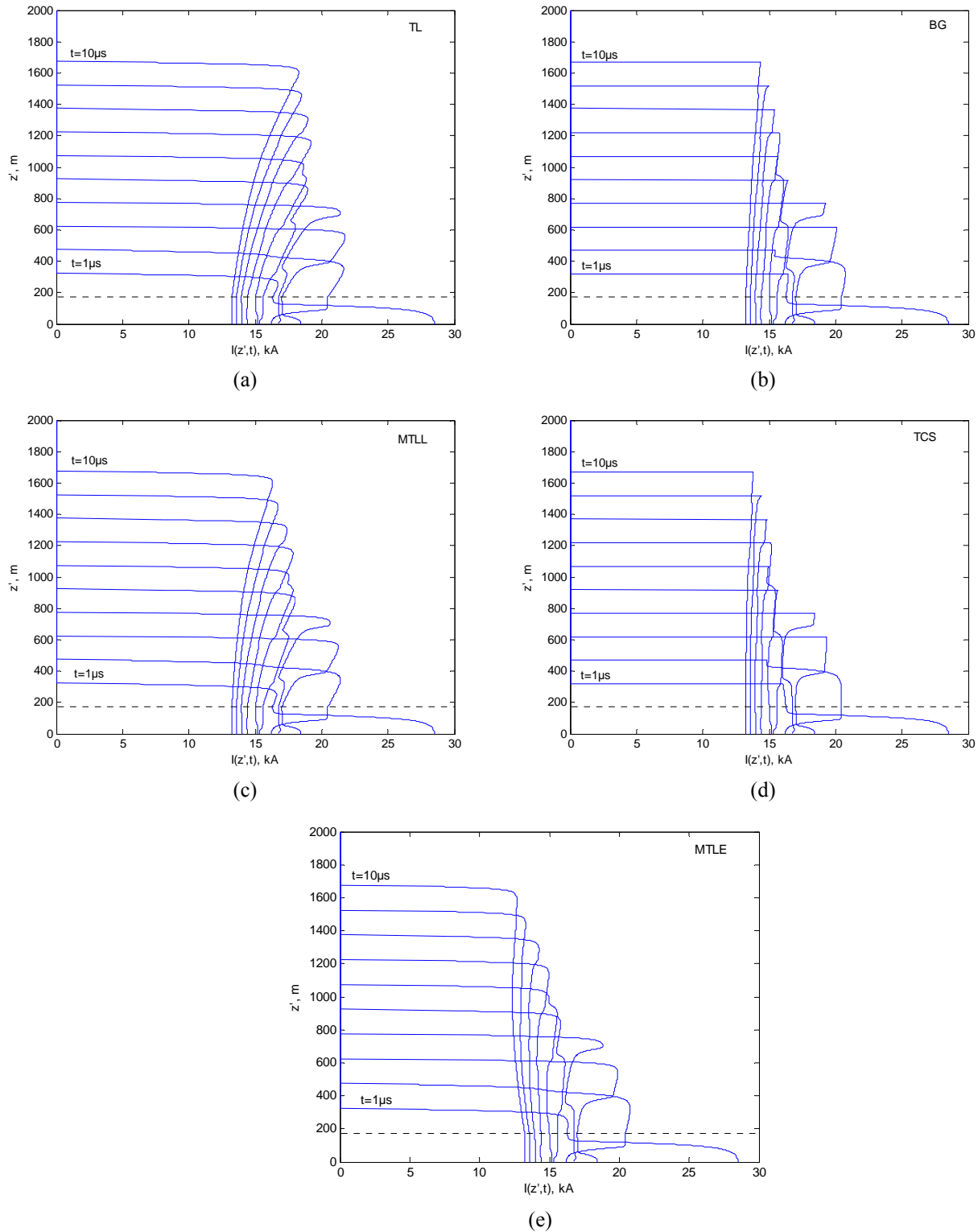


Fig.2 - Current as a function of height z' at ten instants of time, $t=1, 2, \dots, 10 \mu\text{s}$, for five models starting from the same undisturbed current (shown in Fig. 1). (a) TL model, (b) BG model, (c) MTLL model, (d) TCS model, (e) MTLE model.

The horizontal dashed line indicates the height of the tower (168 m). (Adapted from [34])

- although the vertical scale of figure 2 does not allow resolution of current variation at the return stroke wavefront for TL, MTLL and MTLE models, these models have also a discontinuity at the front. This discontinuity arises from the fact that the current injected into the tower at its top is reflected back and forth at its top and bottom ends, and portions of this current are transmitted into the channel; these transmitted pulses, which are assumed to travel at the speed of light, catch up with the return stroke wavefront traveling at a lower speed, but not allowed to propagate in the leader channel above the return stroke front [37].

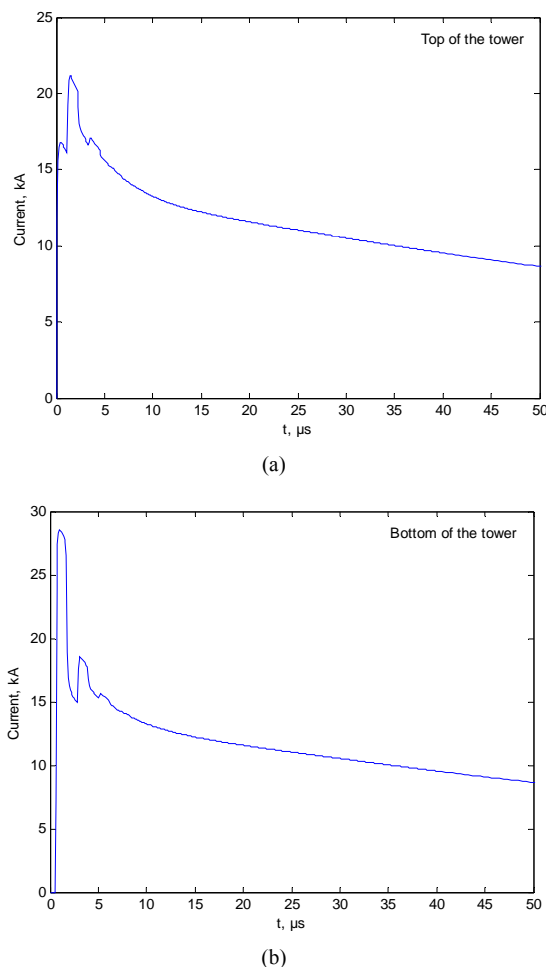


Fig. 3 - Current at the top (a) and at the bottom (b)) of a 168-m tower. (Adapted from [34])

Figure 3 shows the waveforms of current evaluated at the top (168 m) and the base of the tower (0 m). The effects of the multiple reflections at the tower extremities are clearly visible in the waveforms. It can also be seen that the current at the tower base has a

higher peak value due to the contribution from the reflected wave at the ground level [34].

2.5 Determination of reflection coefficients at the top and the bottom of the strike object

Engineering models require that the reflection coefficients at the top and bottom of the strike object be known. In most of the studies, those coefficients are assumed to be constant and frequency-independent. The values of the reflection coefficients have been inferred by several authors from a limited experimental set of current waveforms found in the literature [38-40]. The knowledge of reflection coefficients is also required to extract the 'primary' (or undisturbed) current exempt from the disturbances introduced by the transient processes along the tower. Guerrieri et al. [13] proposed a formula, corrected by Rachidi et al. [3], to extract the undisturbed current. The formula involves an infinite summation in the time domain, assuming that the reflection coefficients are constant and known. Gavric [41] proposed an iterative method based on the Electromagnetic Transient Program (EMTP) to remove superimposed reflections caused by a strike tower from digitally recorded lightning flash currents. Janischewskyj et al. [42] derived reflection coefficients at the CN Tower in Toronto and stated that the values depend on the initial rise time of the measured current, although the limited number of points in their plots render the drawing of conclusions difficult. A dependence on the risetime would suggest that at least one of the reflection coefficients is a function of the frequency. They also proposed a method to extract the reflection coefficients from the measured current waveform. However, their method is applicable only assuming a simplified current waveform (double ramp) and neglecting any frequency dependence for the reflection coefficients. The last consideration was relaxed in a first approximation by Bermudez et al. [23]. They derive a frequency-domain counterpart of expressions (1) and (2) which include the frequency-dependence of reflection coefficients. They also derived an expression to calculate the reflection coefficient as a function of frequency at the bottom of the lightning strike object from two currents measured at different heights along the strike object.

They showed that [23], if the current and its time derivative overlap with reflections at the top or bottom of the strike object, it is impossible to derive the reflection coefficient at the top of the strike object

exactly from any number of simultaneous current measurements. They proposed an extrapolation method to estimate this reflection coefficient. The proposed methodology was applied to experimental data obtained on Peissenberg Tower (Germany) consisting of lightning currents measured at two heights. The obtained results suggest that the reflection coefficient at ground level can be considered as practically constant in the frequency range 100 kHz to 800 kHz [23].

3 ANTENNA THEORY MODELS

3.1 Introduction

An Antenna-Theory-type model was first proposed by Podgorski and Landt in 1985 [4, 43] and it was applied to analyze lightning strikes to the CN Tower. In AT-type models (e.g. [5-7, 44]), the elevated strike object is represented using thin wires and the ground is generally assumed to be perfectly conducting. Very recently, the ground finite conductivity and the buried grounding structure of the tower were included in the analysis [45, 46]. The lightning return-stroke channel is modeled as a vertical wire antenna and the lightning return-stroke current is injected by a voltage source at the tip of the tower. The current distribution along the channel and along the tower is found by solving an electric field integral equation [7].

3.2 Influence of the finite ground conductivity and the buried structure of the tower

Petrache et al. [45, 46] employed the Numerical Electromagnetics Code NEC-4 [47], a well-known and widely used computer code based on the Method of Moments for analyzing the electromagnetic response of antennas and scatterers. Compared to previous NEC versions, such as NEC-2 used by Baba and Ishii [6], NEC-4 is numerically more efficient and can also model wires buried in the ground or penetrating from air into ground. Figure 4 illustrates a wire model for the CN tower adopted by Petrache et al. [45]. Compared to previous models used by Podgorski and Landt [4] and by Kordi et al. [7], structural discontinuities are better reproduced in the present model and furthermore, the grounding structure of the tower is also taken into account as it can be seen in the inset of Fig. 4b. The buried part is composed of 6 vertical wires, each 15-m long. The ground is characterized by its conductivity σ_g and its relative permittivity ϵ_{rg} , assumed to be constant and frequency-independent. In order to reproduce a

return stroke speed along the lightning channel lower than the speed of light, distributed series inductances and resistances are added to the modeled channel [6]. The adopted values are those suggested by Baba and Ishii [6], namely 3 $\mu\text{H/m}$, and 1 Ω/m , respectively. These values correspond to an equivalent return stroke speed of about half the speed of light. The wire structure representing the tower and the lightning channel were divided into 10-m length segments, whereas the underground structure was divided into 1-m length segments. The voltage source at the top of the strike object is determined by the desired current waveform at the channel-base and by the input impedances of the lightning channel and the tower. The detailed procedure is explained in [48] and [7].

Figure 5 presents two current waveforms associated with return-strokes to the CN Tower, which occurred, respectively, on April 7th and April 11th, 1999 [46]. The currents were measured at a height of 509 m. In the same figures, simulation results for the current obtained using NEC-4.

For computations, the source current waveform was specified using Heidler's functions according to the procedure described by Kordi et al. [7]. Comparisons presented in Fig. 5 reveal good agreement between calculated and measured waveforms, especially when the finite ground conductivity is taken into account. In that figure, P.G. stands for perfect ground.

Figure 6 represents the current waveforms in the grounding wires of the tower, at a depth of 5 m below ground, as a function of the ground conductivity. It can be observed that the model-predicted current magnitude is larger for lower ground conductivities. Also, the propagation speed decreases with increasing ground conductivity. Finally, the dispersion effects become more significant and the grounding impedance is expected to decrease for higher values of ground conductivities.

3.3 Reflections from the ground and their dependence on ground conductivity

To analyze the influence of the ground conductivity upon the reflection coefficient at ground level, Petrache et al. [46] considered a simpler tower configuration which is shown in Fig. 7.

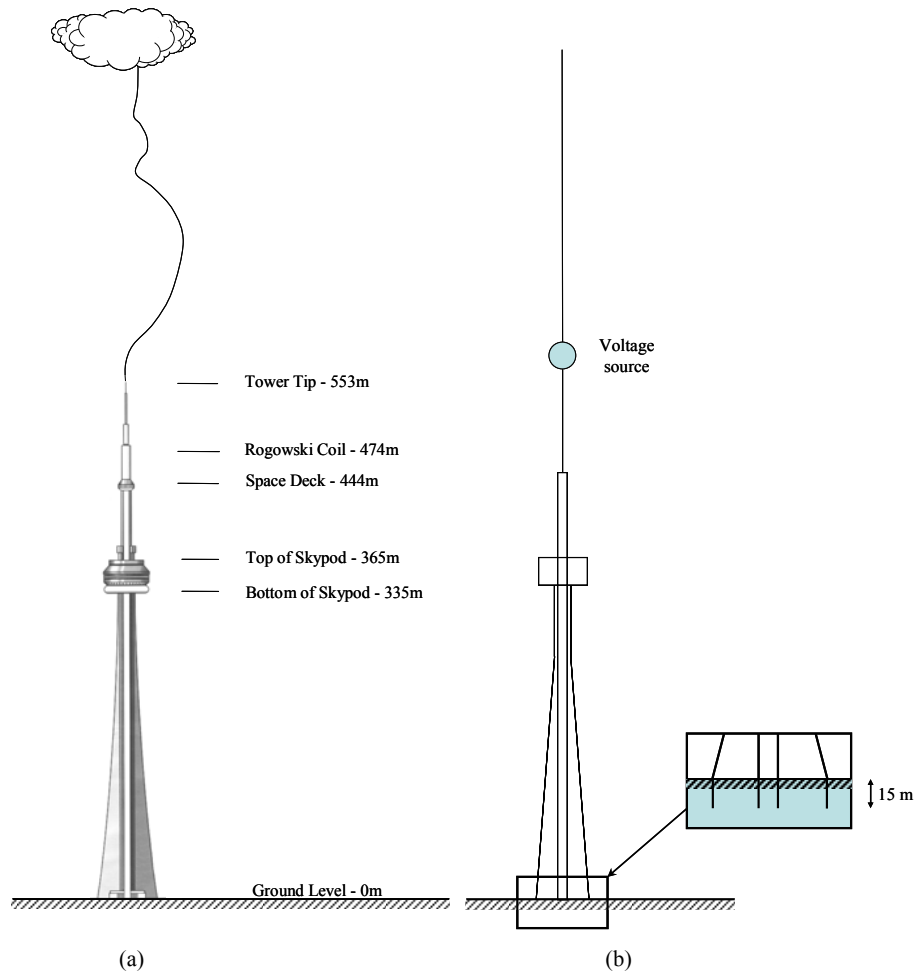


Fig. 4 - (a) The CN Tower, (b) its wire model including its grounding system. (Adapted from [45])

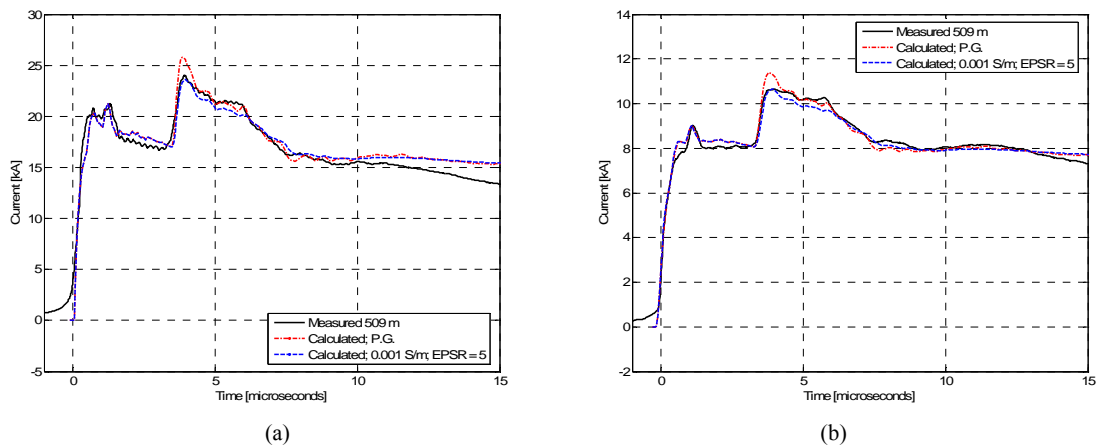


Fig. 5 - Lightning return-stroke currents at a height of 509 m above ground. The measured current waveforms correspond to events recorded at the CN Tower on: (a) April 7th, 1999, first return-stroke; (b) April 11th, 1999, second return-stroke. P.G. stands for perfect ground. (Adapted from [46])

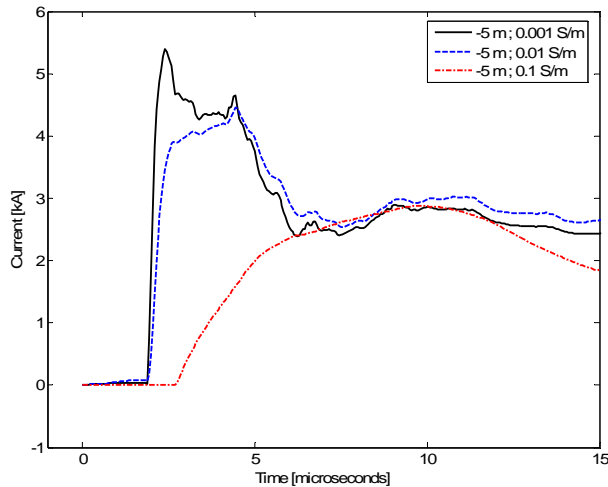


Fig. 6 - Computed lightning return-stroke current waveform in the grounding system of the tower (5m below ground level) as a function of ground conductivity. (Adapted from [45])

They also considered a narrow-width pulse for the incident current (Fig. 8), so as to determine the reflection coefficient in a straightforward way as proposed by Bermudez et al. [23].

Figure 9 shows the simulations for the current at 509 m above ground level and at ground level [46]. The simulations were carried out for different ground conductivities, namely ∞ (perfect ground), 0.01 S/m and 0.001 S/m. The ground's relative permittivity ϵ_{rg} was assumed to be constant and equal to 10.

From Fig. 9, it can be seen that the reflection coefficient at ground level, nearly equal to 1 for a perfectly conducting ground, drops to 0.75 for a ground conductivity of 0.01 S/m and 0.52 for a ground conductivity of 0.001 S/m.

In Fig. 10, one can see the effect of the buried grounding structure of the tower on the current distribution along it. In this Figure, the current waveforms at ground level and at 509 m above ground are presented for a ground conductivity of 0.01 S/m [46]. In Figure 10, a curve is presented for each one of three different grounding arrangements, namely (1) no buried part present, that is the tower is connected to the ground and the underground structure of the tower is not taken into consideration, (2) 15-m long buried structure, and (3) 30-m length buried structure. It can be seen that, for the considered configuration, the grounding structure of the tower does not significantly

affect the current distribution. However, it is worth noting that for other configurations involving lower values of the ground conductivity and/or different grounding structure and length, the effect could be more significant.

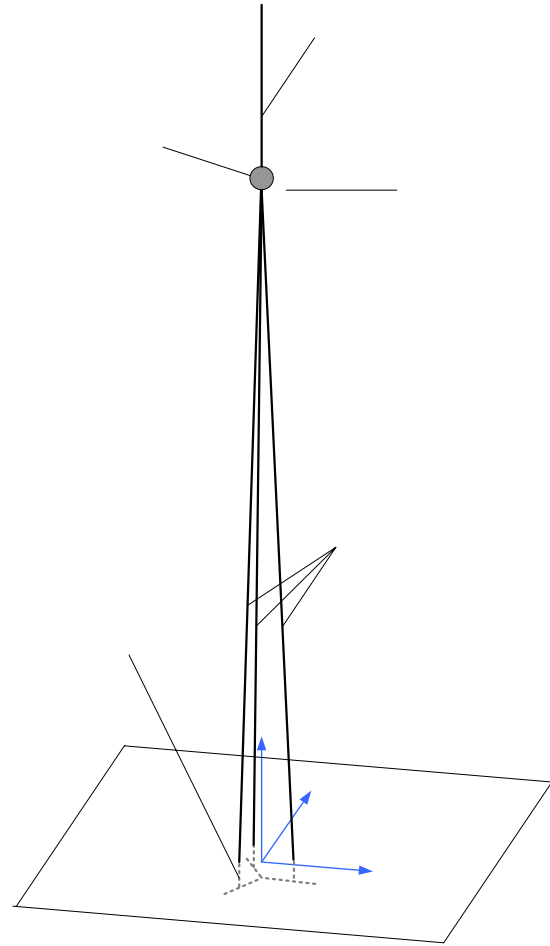


Fig. 7 - Model of the tower used for the analysis of ground reflections. (Adapted from [46])

4 ELECTROMAGNETIC FIELDS

4.1 Electromagnetic field expressions for a perfectly conducting ground and the turn-on term

According to Eq. (1), at a generic height z' along the channel, the current results from the contribution of a series of time-delayed current components. The first one, moving upward at a constant speed v , represents the return stroke wave front which progressively turns on the distributed current sources [3] by way of which the channel is modeled.

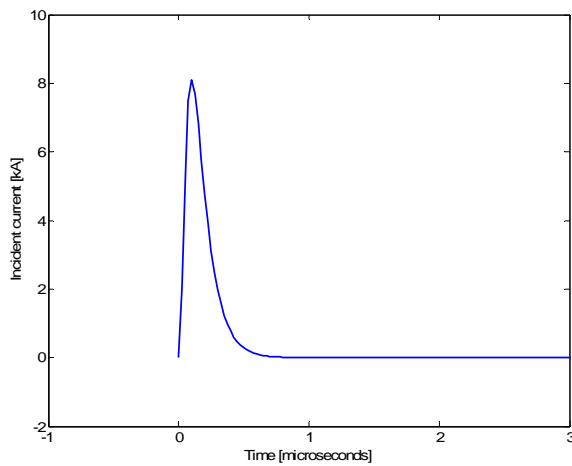
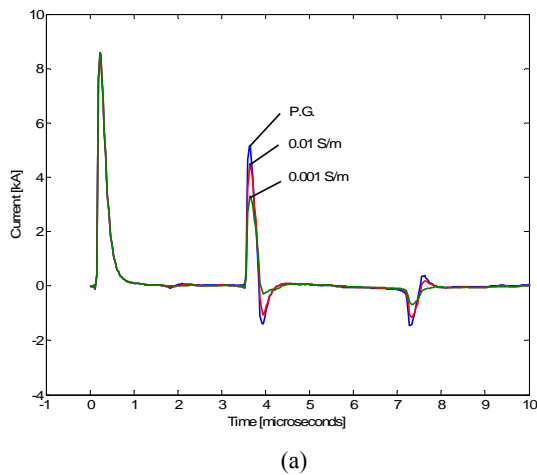
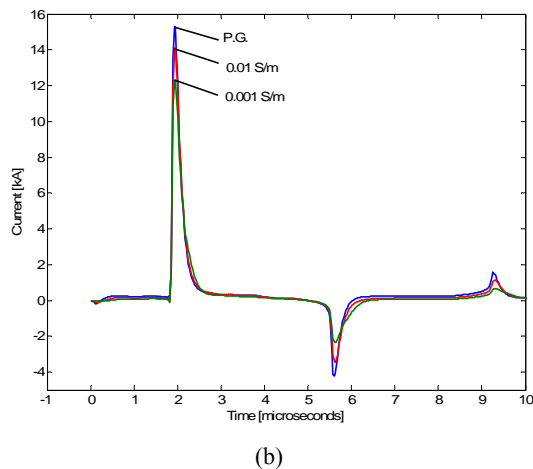


Fig. 8 - Narrow-width pulse incident current. (Adapted from [46])

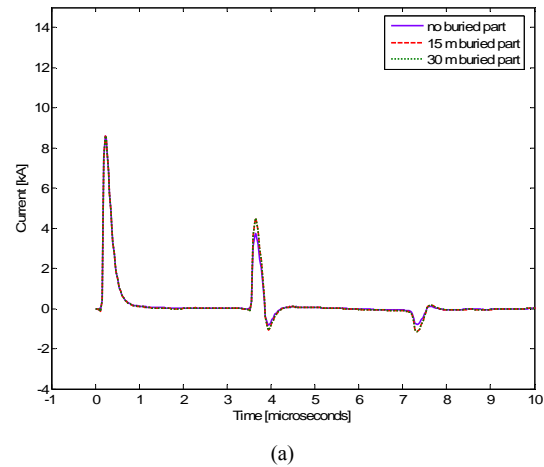


(a)

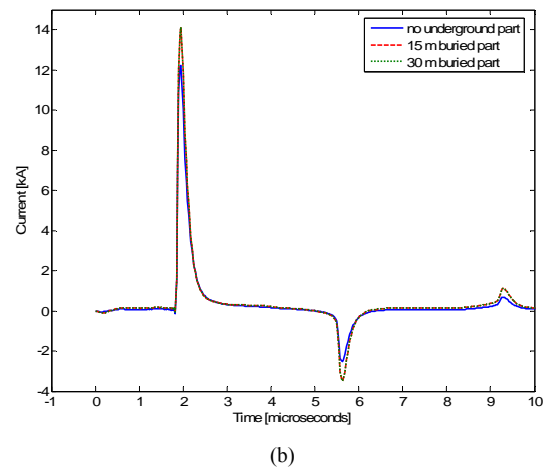


(b)

Fig. 9 - Current at two heights along the tower as a function of the ground conductivity: (a) 509 m, and (b) 0 m (ground level). The incident current is represented in Fig. 8. (Adapted from [46])



(a)



(b)

Fig. 10 - Current at two heights along the tower, (a) at 509 m and (b) at 0 m (ground level), for a ground conductivity of 0.01 S/m and various underground structures. The incident current is represented in Fig. 8. The two curves for 15-m and 30-m buried structure are nearly identical. (Adapted from [46])

Assuming that no current flow is possible above the return stroke wave front, the current distribution has to be abruptly cut off at this front [37, 49]. This is mathematically expressed by the Heaviside function present in Eq. (1).

All other contributions resulting from multiple reflections at the two ends of the tall structure, are supposed to travel at the speed of light. Because of their higher speed, they catch up with the return stroke wave front providing a nonzero contribution which leads to a discontinuity if no current is admitted above the front. Notice that this truncation already produces a discontinuity at time $t=0^+$ since the contribution of the very first distributed current source in the channel is reflected from the tower top and propagates upward at the speed of light [37].

Although such a discontinuity may not be conceivable from a physical point of view, it must still be considered in the analysis for the sake of consistency with the adopted engineering models.

The electromagnetic field contributions from an elemental dipole of current $i(z', t)$ of length dz' located along the vertical axis at z' (see Fig. 11) are calculated with the usual expressions valid for a perfectly conducting ground (e.g. [50]):

$$dE_z(r, z, z', t) = \frac{dz'}{4\pi\epsilon_0} \left[\frac{2(z-z')^2 - r^2}{R^5} \int_{R/c}^t i(z', \tau - R/c) d\tau + \frac{2(z-z')^2 - r^2}{cR^4} i(z', t - R/c) - \frac{r^2}{c^2 R^3} \frac{\partial i(z', t - R/c)}{\partial t} \right] \quad (7)$$

$$dE_r(r, z, z', t) = \frac{dz'}{4\pi\epsilon_0} \left[\frac{3r(z-z')}{R^5} \int_{R/c}^t i(z', \tau - R/c) d\tau + \frac{3r(z-z')}{cR^4} i(z', t - R/c) + \frac{r(z-z')}{c^2 R^3} \frac{\partial i(z', t - R/c)}{\partial t} \right] \quad (8)$$

$$dH_\phi(r, z, z', t) = \frac{dz'}{4\pi} \left[\frac{r}{R^3} i(z', t - R/c) + \frac{r}{cR^2} \frac{\partial i(z', t - R/c)}{\partial t} \right] \quad (9)$$

in which

- r, z are the cylindrical coordinates of the observation point,
- R is the distance between the dipole and the observation point, $R = \sqrt{r^2 + (z-z')^2}$,
- $i(z', t)$ is the dipole current,
- c is the speed of light, and,
- ϵ_0 is the permittivity of free space.

The total electromagnetic fields are calculated by integrating the above equations along the tower-channel and its image, assuming a perfectly-conducting ground.

In the presence of a current discontinuity, the radiation term, namely the last term in each equation, introduces a singularity that needs to be treated separately [50-55].

The complete expression of the electromagnetic field is obtained by integrating (7) through (9) along z' from ground level to the wave front and then by adding the corrective turn-on term across the discontinuity in H , expressed as

$$\int_H f(z', z, r) \frac{\partial i(z', t - R/c)}{\partial t} dz' \quad (10)$$

where $f(z', z, r)$ can be $r^2/c^2 R^3$, $r(z-z')/c^2 R^3$ or r/cR^2 , depending on which component of the field is being calculated [37].

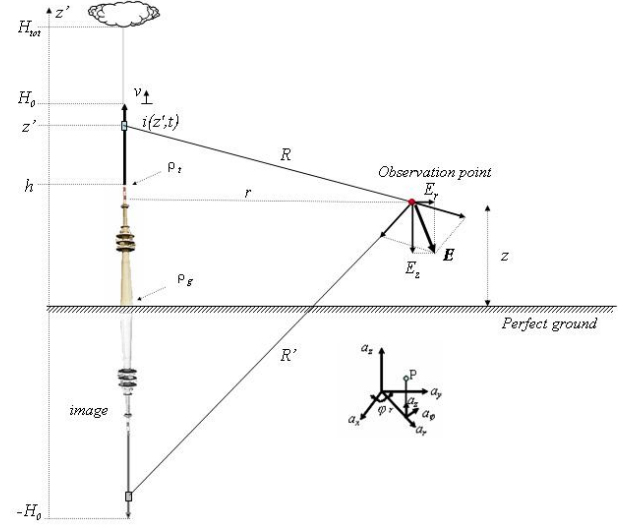


Fig. 11 – Adopted geometry for field computation [49]

The reason why an additional turn-on term must be introduced in the field equations is that the presence of the Heaviside function in Eq. (1) cannot be disregarded when the time-derivative of the current is calculated. Its derivative, namely, a delta function, multiplied by the amplitude of the current at the wave front, needs to be

added to the radiation term. In the case in which the current distribution presents no discontinuity at the return stroke wave front, this turn-on term contribution vanishes. The discontinuity can be treated considering a nondiscontinuous current wave front of length $\Delta z''$ which reaches the level I_{front} linearly in a time Δt , and expressing the radiation integral across H taking the limit when the front duration tends to zero [50].

The final expressions for the turn-on term fields, in which the apparent front speed appears as the reciprocal of the term between brackets are given by [37]:

$$H_{\Phi / \text{turn-on}} = \frac{I_{front}(H) \cdot r}{4\pi c R^2} \cdot \frac{1}{\left[\frac{1}{v} - \frac{(z-H)}{cR} \right]} + \frac{I_{front}(H') \cdot r}{4\pi c R'^2} \cdot \frac{1}{\left[\frac{1}{v} - \frac{(z-H')}{cR'} \right]} \quad (11)$$

$$E_{r / \text{turn-on}} = \frac{I_{front}(H) \cdot r \cdot (z-H)}{4\pi \epsilon_0 c^2 R^3} \cdot \frac{1}{\left[\frac{1}{v} - \frac{(z-H)}{cR} \right]} + \frac{I_{front}(H') \cdot r \cdot (z-H')}{4\pi \epsilon_0 c^2 R'^3} \cdot \frac{1}{\left[\frac{1}{v} - \frac{(z-H')}{cR'} \right]} \quad (12)$$

$$E_{z/turn-on} = -\frac{I_{front}(H) \cdot r^2}{4\pi\epsilon_0 c^2 R^3} \cdot \frac{1}{\left[\frac{1}{v} - \frac{(z-H)}{cR}\right]} + \quad (13)$$

$$-\frac{I_{front}(H') \cdot r^2}{4\pi\epsilon_0 c^2 R'^3} \cdot \frac{1}{\left[\frac{1}{v} - \frac{(z-H')}{cR'}\right]}$$

In equations (11)-(13), the two terms on the right-hand side represent the turn-on term due to the discontinuity at the wavefront and at its image, respectively.

The general expression for the current at the wavefront is simply obtained from Eq. (1) in which the time variable t appears implicitly through H [37]:

$$I_{front}(H) = P(H-h) i_0 \left(h, \frac{H-h}{v} + \frac{1}{c} \sqrt{r^2 + (H-z)^2} - \frac{H-h}{v^*} \right) +$$

$$- \rho_i i_0 \left(h, \frac{H-h}{v} + \frac{1}{c} \sqrt{r^2 + (H-z)^2} - \frac{H-h}{c} \right) +$$

$$+ (1 - \rho_i)(1 + \rho_i) \sum_{n=0}^{\infty} \rho_g^{n+1} \rho_i^n i_0 \left(h, \frac{H-h}{v} + \frac{1}{c} \sqrt{r^2 + (H-z)^2} - \frac{H+h}{c} - \frac{2nh}{c} \right) \quad (14)$$

It is worth to observe that the first term on the right-hand side of Eq. (14) is nonzero only for the BG and TCS models, and it corresponds to the inherent discontinuity predicted by these two models. This means, by consequence, that the turn-on term has the same expression for the TL, MTLL and MTLE models [37].

The contribution of the turn-on term to the total field depends on many factors such as the height of the tower, the reflection coefficients at its extremities, the return stroke speed and the position of the observation point (distance and elevation). Pavanello et al. [37] found that the contribution of the turn on term to the total electric and magnetic fields is negligible at close distances (below 100 m) and increases rapidly to reach an asymptotic value of about 12% at a distance of 5 km and beyond. At these distances, the field peak is essentially due to the radiation term.

4.2 Comparison between different engineering models

Pavanello et al. [34] compared five engineering models (BG, TCS, TL, MTLL and MTLE) employing the same undisturbed current $i_0(t)$, presented in Fig. 1. The elevated strike object was assumed to have a height $h=168$ m, corresponding to the Peissenberg tower in Germany.

The reflection coefficients are set respectively to $\rho_t = -0.53$ and $\rho_g = 0.7$ [36].

Figure 12 presents electric and magnetic fields calculated at a distance of 50 m from the tower base [34]. At this distance, the electric field is dominated (at later times) by its electrostatic term. The model-predicted electric fields are very similar for the first 5 μ s, beyond which the BG, TCS and MTLL models predict the flattening of the field, typically observed at close distances, while the TL model predicts a field decay. The late-time E-field predicted by the MTLE model exhibits a ramp, as in the case of a ground-initiated return stroke [34]. Note, however, that a judicious choice of the attenuation factor would result in the flattening of the late-time E-field at close range [56].

Figure 12b shows that the predicted magnetic field is nearly model-independent. At this distance, the magnetic field is dominated by its induction term, and its waveshape is similar to the current at the base of the tower shown in Fig. 3b.

Figure 13 presents calculated electric and magnetic fields at a distance of 5 km [34]. The electric and magnetic field waveshapes for the first 5 μ s are dominated by the radiation term and hence they are very similar. No significant differences are found between the various models in this early-time region. The differences between the model predictions become more pronounced at late times, $t > 5$ μ s or so, although they are unremarkable. Note that all the models predict flattening of the electric field at later times at a value that is significantly smaller than the initial peak, in contrast with calculated electric fields for ground-initiated return strokes (see, for example, Fig. 12 of [35]).

The electric and magnetic fields at a distance of 100 km are plotted in Figure 14 [34]. At this distance, the fields are essentially radiation fields, and electric and magnetic fields have the same waveshape. The fields associated with ground-initiated return strokes at such distances exhibit a zero-crossing which is only reproduced by the MTLE and MTLL models [2, 35]. As seen in figure 14, for the considered case of a 168-m tower-initiated return stroke, none of the models predicts a zero-crossing. The absence of zero-crossing, in particular for the MTLE and MTLL models, can be explained by the contribution of the turn-on term [37].

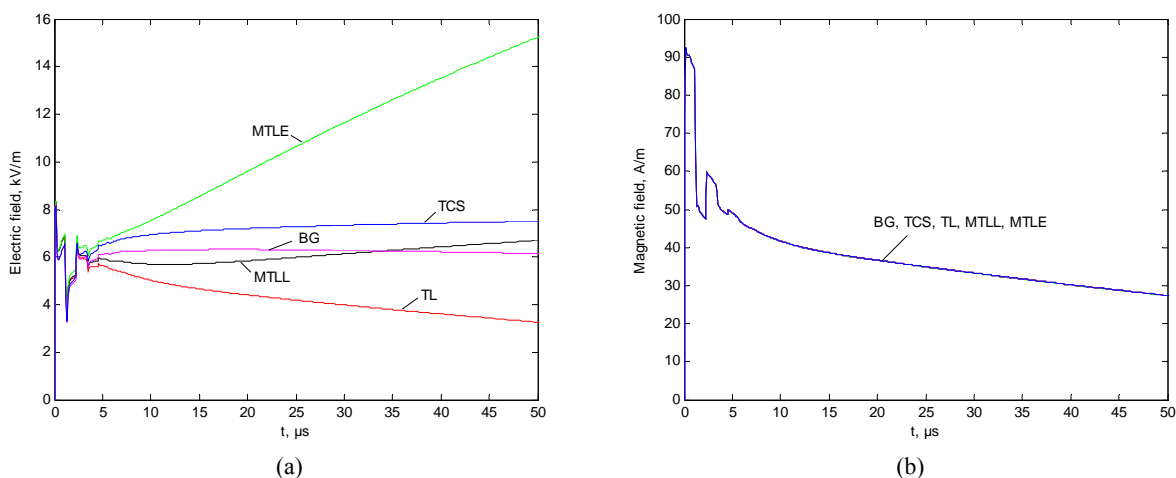


Fig. 12 - Electric (a) and magnetic (b) fields calculated at a distance of 50 m from a lightning return stroke to a 168-m tower. (Adapted from [34])

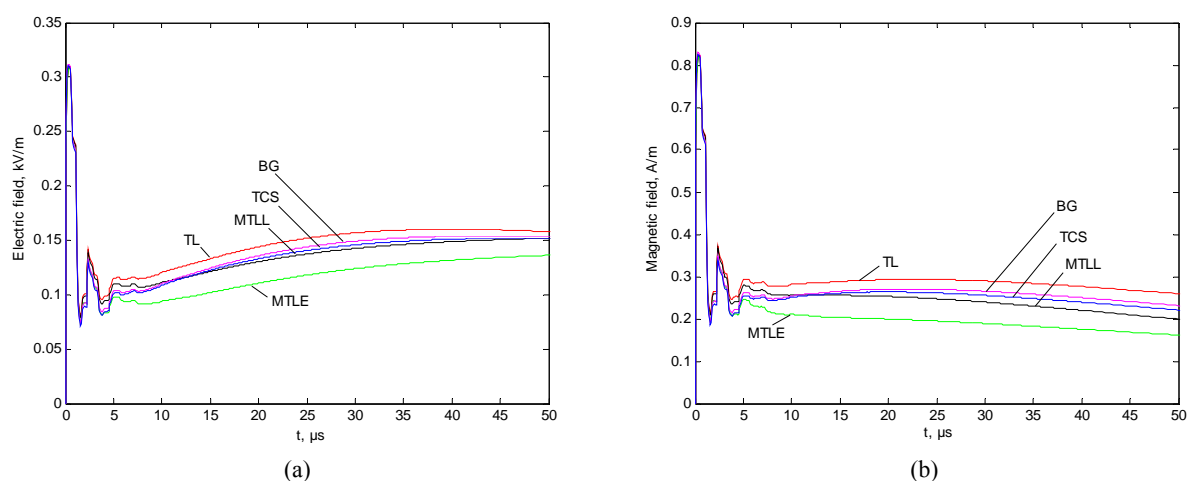


Fig. 13 - Electric (a) and magnetic (b) fields calculated at a distance of 5 km from a lightning return stroke to a 168-m tower. (Adapted from [34])

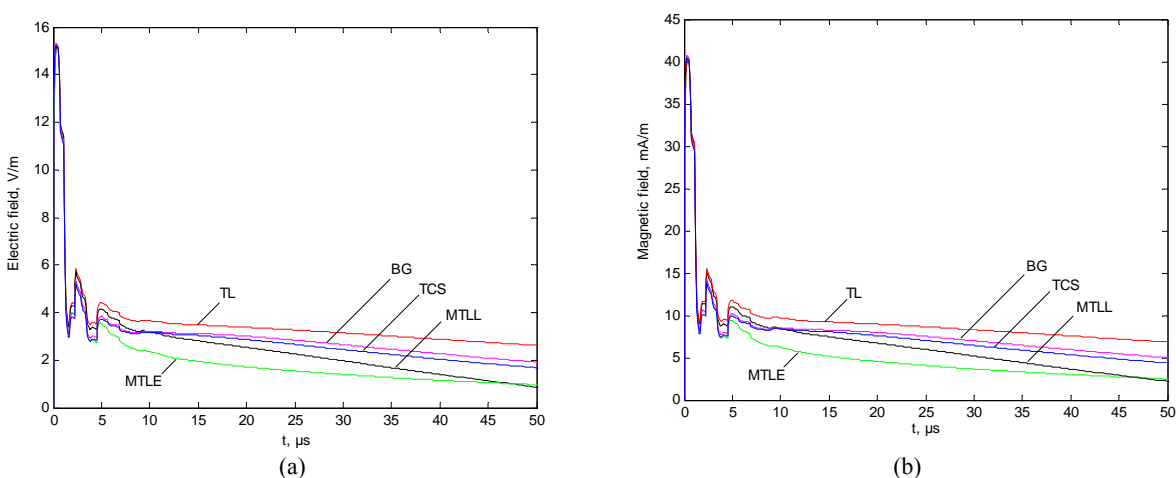


Fig. 14 - Electric (a) and magnetic (b) fields calculated at a distance of 100 km from a lightning return stroke to a 168-m tower. (Adapted from [34])

4.3 Propagation effects

The effect of the finite conductivity of the ground on the amplitude and waveshape of electromagnetic fields radiated by lightning return strokes to tall towers was recently investigated in [57]. The study was based on the engineering return stroke models extended to take into account the presence of a vertically-extended strike object. In [57], the propagation along a finitely-conducting ground is taken into account using Cooray's approach [58]. Simulations were presented for a homogeneous ground and considering three cases: (1) a return stroke initiated at ground level, (2) a return stroke to a 168-m tall tower corresponding to the Peissenberg tower, and (3) a return stroke to a 553-m tall tower corresponding to the CN Tower. It is shown that the propagation along an imperfectly conducting ground causes the amplitude of the field to decrease and its risetime to increase with decreasing ground conductivity. In addition, it was found that some of the fine structure of the electromagnetic field associated with transient processes along the struck tower vanishes due to propagation effects. Simulations presented in [57] revealed also that the enhancement effect of the tower (with respect to a ground-initiated return stroke) on the peak field, which is considerable for a perfectly conducting ground, tends to become less significant for a lossy ground.

4.4 Effect of the tower

Based on theoretical modeling and experimental observations, it is well established that the presence of a tower could result in a substantial increase (a factor of 3 or so) of the electric and magnetic field peaks and their derivatives (e.g. [17, 24, 25]) for observation points located at distances exceeding the height of the tower.

Interestingly, the effect of the tower at distances of about the height or the tower or less, could result in a significant decrease of the electric field (e.g. [25, 59, 60]).

5 CONCLUSIONS AND PERSPECTIVES

The presence of an elevated strike object have been included in two types -or classes- of return stroke models, namely the engineering models and the electromagnetic or Antenna-Theory (AT) models. In the engineering return stroke models, the spatial and temporal distribution of the channel current is specified based on observed characteristics such as channel-base

current, return stroke speed and remote electromagnetic fields. The presence of an elevated strike object in such models have been considered by assuming the object as a uniform, lossless transmission line. In Antenna-Theory-type models, the strike object and the lightning channel are represented using thin wires. The Maxwell's equations are numerically solved using the method of moments to find the current distribution along the lightning channel, from which the radiated electromagnetic fields can be computed.

For engineering models, the current profile along the channel and along the strike object, as well as radiated electric and magnetic fields at different distances, predicted by various models (BG, TCS, TL, MTLL and MTLE) have been presented and discussed. The current distribution associated with these engineering extended models exhibits a discontinuity at the return stroke wave front that needs to be represented by an additional term, the so-called "turn-on" term, in the well-known field equations. Regarding the radiated field, except for the case of very close (50 m) electric field, it is found that the computed electromagnetic fields associated with a strike to a 168-m tall tower are less model-dependent than those corresponding to a strike to ground. In addition, it is found that none of the models predicts the zero crossing of the field at far distances, a typically-observed feature for ground-initiated lightning return strokes. Experimental data at these distances are needed to confirm whether far field zero crossing is indeed absent for tower-initiated return strokes.

An analysis of lightning return-strokes to tall structures was presented using AT model, in which the finite ground conductivity as well as the buried grounding system of the tall structure were taken into account. It is shown that, although the finite ground conductivity has a minor effect on the current distribution along the struck tower, the current waveform in sections of the tower close to ground is somewhat affected by finite ground conductivity. Furthermore, the simulations show that some fine structure in the measured current waveforms along the CN Tower can be attributed to the finite ground conductivity. In addition, simulation results suggest that the reflection coefficient at ground level is strongly affected by the finite ground conductivity.

The research performed by different research groups in the last 5 years or so has raised some important

questions that need to be elucidated by further theoretical investigations and experimental measurements. Some of these issues are the following

- Does the distant electromagnetic field radiated by a strike to tall tower feature an inversion of polarity which is until now believed to be a fundamental characteristic of lightning radiation fields and which is used as one of the basic criteria for the remote identification of lightning? Or, as suggested by recent theoretical analyses, such an inversion of polarity does not occur in the tens of microsecond range for lightning strikes to the tower.
- What is the influence of the height of the strike object on the return stroke current inferred from remote field measurements? Recent analysis has shown that the enhancement/attenuation of the electromagnetic field depends on the height of the tower. Specific equations have been derived for both tall and short towers which need to be further tested.
- The vertical strike object is generally represented by a uniform transmission line. The adequacy of such a representation has been recently questioned in some studies. It is suggested that this model could fail in reproducing electric fields in the immediate vicinity of the tower.

6 ACKNOWLEDGEMENT

This paper is based on an invited lecture presented at the SIPDA'05 Conference. Most of the results reported in this lecture are obtained within the framework of an international collaboration involving Swiss Federal Institute of Technology (Lausanne, Switzerland), Universities of Bologna and Rome (Italy), Universities of Toronto and Mc Master (Canada), University of Florida (USA) and others. The author expresses his sincere gratitude to J.L. Bermudez, C.A. Nucci, V.A. Rakov, M. Rubinstein and D. Pavanello for their valuable contributions, comments and suggestions. The author is also grateful to A. Borghetti, J.S. Chang, W.A. Chisholm, V. Cooray, G. Diendorfer, Z. Flisowski, F. Heidler, S. Guerrieri, A.M. Hussein, M. Ianoz, W. Janischewskyj, B. Kordi, E.P. Krider, C. Mazzetti, R. Moini, E. Petrache, M. Paolone, T. Shindo, V. Shostak, W. Schulz, F.M. Tesche, N. Theethayi, R. Thottappillil, M.A. Uman, and S. Yokoyama for interesting and fruitful discussions on the subject over the last two decades or so. This work was partially done within the European COST Action P18 (The Physics of Lightning Flash and its Effects) and was funded by the Swiss National Science Foundation (Grant No 2000-068147) and by the Swiss State Secretariat for Education and Research SER (Grant No C05.0149).

7 REFERENCES

1. Rakov, V.A., *Transient response of a tall object to lightning*. IEEE Transactions on Electromagnetic Compatibility, 2001. **43**(4): p. 654-61.
2. Rakov, V.A. and M.A. Uman, *Review and evaluation of lightning return stroke models including some aspects of their application*. IEEE Transactions on Electromagnetic Compatibility, 1998. **40**(4): p. 403-26.
3. Rachidi, F., et al., *The Effect of Vertically-Extended Strike Object on the Distribution of Current Along the Lightning Channel*. Journal of Geophysical Research, 2002. **107**(D23): p. 4699.
4. Podgorski, A.S. and J.A. Landt. *Numerical analysis of the lightning-CN tower interaction*. in *6th Symposium and Technical Exhibition on Electromagnetic Compatibility*. 1985. Zurich, Switzerland.
5. Heidler, F. and T. Zundl. *Influence of tall towers on the return stroke current*. in *Aerospace and Ground Conference on Lightning and Static Electricity*. 1995. Williamsburg, USA.
6. Baba, Y. and M. Ishii, *Numerical electromagnetic field analysis of lightning current in tall structures*. IEEE Transactions on Power Delivery, 2001. **16**(2): p. 324-8.
7. Kordi, B., et al., *Application of the antenna theory model to a tall tower struck by lightning*. Journal of Geophysical Research, 2003. **108**(D17).
8. Harrington, R.F., *Field computation by Moment Methods*. 1993, New York: IEEE & Wiley.
9. Visacro, S. and F.H. Silveira, *Evaluation of lightning current distribution along the lightning discharge channel by a hybrid electromagnetic model*. Journal of Electrostatics, 2004. **60**: p. 111-120.
10. Silveira, F.H., S. Visacro, and A.R. De Conti. *Lightning effects on the vicinity of elevated structures*. in *International Conference on Lightning Protection ICLP*. 2004. Avignon, France.
11. Zundl, T. *Lightning current and LEMP calculations compared to measurements gained at the Peissenberg tower*. in *22nd ICLP (International Conference on Lightning Protection)*. 1994. Budapest, Hungary.
12. Guerrieri, S., et al., *Extension of two return stroke models to consider the influence of elevated strike objects on the lightning return stroke current and the radiated electromagnetic field: comparison with experimental results*. EMC '96 ROMA. International Symposium on Electromagnetic Compatibility. Univ. Rome 'La Sapienza', Rome, Italy, 1996. **2**.
13. Guerrieri, S., et al., *On the influence of elevated strike objects on directly measured and indirectly estimated lightning currents*. IEEE Transactions on Power Delivery, 1998. **13**(4): p. 1543-55.
14. Guerrieri, S., E.P. Krider, and C.A. Nucci. *Effects of Traveling-Waves of Current on the Initial Response of a Tall Franklin Rod*. in *ICLP2000*. 2000. Rhode, Greece.
15. Rusan, I., et al. *Comparison of measured and computed electromagnetic fields radiated from lightning strikes to*

- the Toronto CN tower. in *23rd International Conference on Lightning Protection (ICLP)*. 1996. Florence.
16. Motoyama, H., et al., *Electromagnetic field radiation model for lightning strokes to tall structures*. IEEE Transactions on Power Delivery, 1996. **11**(3): p. 1624-32.
 17. Rachidi, F., et al., *Current and electromagnetic field associated with lightning return strokes to tall towers*. IEEE Trans. on Electromagnetic Compatibility, 2001. **43**(3).
 18. Janischewskyj, W., V. Shostak, and A.M. Hussein. *Comparison of lightning electromagnetic field characteristics of first and subsequent return strokes to a tall tower 1. Magnetic field*. in *24th ICLP (international conference on lightning Protection)*. 1998. Birmingham, U.K.
 19. Janischewskyj, W., V. Shostak, and A.M. Hussein, *Lightning electric field characteristics of first and subsequent return strokes to a tall tower*. Eleventh International Symposium on High Voltage Engineering, 1999. **467**(5).
 20. Shostak, V., et al. *Electromagnetic fields of lightning strikes to a tall tower: a model that accounts for upward-connecting discharges*. in *25th ICLP (International Conference on Lightning Protection)*. 2000. Rhodes, Greece.
 21. Shostak, V., et al. *Return-stroke current modeling of lightning striking a tall tower accounting for reflections within the growing channel and for upward-connecting discharges*. in *11th International Conference on Atmospheric Electricity*. 1999. Guntersville, U.S.A.
 22. Goshima, H., et al., *Characteristics of electromagnetic fields due to winter lightning stroke current to a high stack*. Transactions of the Institute of Electrical Engineers of Japan, Part B, 2000. **120**(1): p. 44-9.
 23. Bermudez, J.L., et al., *Determination of Reflection Coefficients at the Top and Bottom of Elevated Strike Objects Struck by Lightning*. Journal of Geophysical Research, 2003. **108**(D14): p. 4413, doi: 10.1029/2002JD002973.
 24. Bermudez, J.L., et al., *Far-field - current relationship based on the TL model for lightning return strokes to elevated strike objects*. IEEE Transactions on Electromagnetic Compatibility, 2005. **47**(1): p. 146-159.
 25. Baba, Y. and V.A. Rakov, *Lightning electromagnetic environment in the presence of a tall grounded strike object*. Journal of Geophysical Research, 2005. **110**.
 26. Rusan, R., et al. *Comparison of measured and computed electromagnetic fields radiated from lightning strikes to the Toronto CN tower*. in *23rd ICLP (International Conference on Lightning Protection)*. 1996. Florence, Italy.
 27. Rachidi, F. and C.A. Nucci, *On the Master, Uman, Lin, Sandler and the Modified Transmission Line lightning return stroke current models*. Journal of Geophysical Research, 1990. **95**(D12): p. 20389-94.
 28. Cooray, G.V., *On the concepts used in return stroke models applied in engineering practice*. IEEE Trans. on Electromagnetic Compatibility, 2002. **45**(1): p. 101-108.
 29. Baba, Y. and V.A. Rakov, *On the use of lumped sources in lightning return stroke models*. Journal of Geophysical Research, 2005. **110**.
 30. Shostak, V., et al. *Modeling of the electromagnetic field associated with lightning return strokes to a complex tall tower*. in *26th ICLP (International Conference on Lightning Protection)*. 2002. Cracow, Poland.
 31. Shostak, V., W. Janischewskyj, and A.M. Hussein. *Expanding the modified transmission line model to account for reflections within the continuously growing lightning return stroke channel*. in *IEEE Power Engineering Society Summer Meeting*. 2000. Piscataway, USA: Cat. IEEE.
 32. Bermudez, J.L., et al. *On the use of transmission line theory to represent a nonuniform vertically-extended object struck by lightning*. in *2003 IEEE Symposium on Electromagnetic Compatibility (EMC)*. 2003. Boston, USA.
 33. Baba, Y. and V.A. Rakov, *On the interpretation of ground reflections observed in small-scale experiments simulating lightning strikes to towers*. IEEE Transactions on Electromagnetic Compatibility, 2005. **47**(3).
 34. Pavanello, D., et al. *Return Stroke Current Profiles and Electromagnetic Fields Associated with Lightning Strikes to Tall Towers: Comparison of Engineering Models*. in *International Conference on Lightning Protection, ICLP 2004*. 2004. Avignon, France.
 35. Nucci, C.A., et al., *Lightning return stroke current models with specified channel-base current: a review and comparison*. Journal of Geophysical Research, 1990. **95**(D12): p. 20395-408.
 36. Heidler, F., J. Wiesinger, and W. Zischank. *Lightning Currents Measured at a Telecommunication Tower from 1992 to 1998*. in *14th International Zurich Symposium on Electromagnetic Compatibility*. 2001. Zurich, Switzerland.
 37. Pavanello, D., et al., *Electromagnetic Field Radiated by Lightning to Tall Towers: Treatment of the Discontinuity at the Return Stroke Wavefront*. Journal of Geophysical Research, 2004. **109**(D06114).
 38. Beierl, O. *Front Shape Parameters of Negative Subsequent Strokes Measured at the Peissenberg Tower*. in *21st ICLP (International Conference on Lightning Protection)*. 1992. Berlin, Germany.
 39. Montandon, E. and B. Beyeler. *The Lightning Measuring Equipment on the Swiss PTT Telecommunications Tower at St. Chrischona, Switzerland*. in *22nd ICLP (International Conference on Lightning Protection)*. 1994. Budapest, Hungary.
 40. Willett, J.C., et al., *An experimental test of the 'transmission-line model' of electromagnetic radiation*

- from triggered lightning return strokes. *Journal of Geophysical Research*, 1988. **93**(D4): p. 3867-78.
41. Gavric, M.R., *Iterative method for waveshape restoration of directly measured lightning flash currents*. IEE Proceedings Generation, Transmission and Distribution, 2002. **149**(1): p. 66-70.
 42. Janischewskyj, W., et al. *Collection and use of lightning return stroke parameters taking into account characteristics of the struck object*. in *23rd ICLP (International Conference on Lightning Protection)*. 1996. Florence, Italy.
 43. Podgorski, A.S. and J.A. Landt, *Three dimensional time domain modelling of lightning*. *IEEE Transactions on Power Delivery*, 1987. **PWRD-2**(3): p. 931-938.
 44. Moini, R., et al. *An antenna theory model for the lightning return stroke*. in *12th International Zurich Symposium on Electromagnetic Compatibility*. 1997. Zurich, Switzerland.
 45. Petrache, E., et al. *Lightning Strikes to Elevated Structures: Influence of Grounding Conditions on Currents and Electromagnetic Fields*. in *IEEE International Symposium on Electromagnetic Compatibility*. 2005. Chicago.
 46. Petrache, E., et al. *Influence of the finite ground conductivity on the transient response to lightning of a tower and its grounding*. in *28th General Assembly of International Union of Radio Science (URSI)*. 2005. New Delhi, India.
 47. Burke, G.J., *Numerical Electromagnetics Code NEC-4 Method of Moments*. 1992, Lawrence Livermore National Laboratory.
 48. Moini, R., et al., *A new lightning return stroke model based on antenna theory*. *Journal of Geophysical Research*, 2000. **105**(D24): p. 29693-702.
 49. Pavanello, D., et al. *On the calculation of Electromagnetic Fields Radiated by Lightning to Tall Structures*. in *International Conference on Lightning Protection, ICLP 2004*. 2004. Avignon, France.
 50. Rubinstein, M. and M.A. Uman, *Transient electric and magnetic fields associated with establishing a finite electrostatic dipole, revisited*. *IEEE Transactions on Electromagnetic Compatibility*, 1991. **33**(4): p. 312-20.
 51. Rubinstein, M. and M.A. Uman, *On the radiation field turn-on term associated with traveling current discontinuities in lightning*. *Journal of Geophysical Research*, 1990. **95**(D4): p. 3711-13.
 52. Le Vine, D.M. and J.C. Willett, *Comment on the transmission line model for computing radiation from lightning*. *Journal of Geophysical Research*, 1992. **97**: p. 2601-2610.
 53. Thottappillil, R. and V.A. Rakov, *On different approaches to calculating lightning electric fields*. *Journal of Geophysical Research*, 2001. **106**: p. 14191-14205.
 54. Thottappillil, R., V. Rakov, and M. Uman, *Distribution of charge along the lightning channel: relation to remote electric and magnetic fields and to return-stroke models*. *Journal of Geophysical Research*, 1997. **102**(D6): p. 6987-7006.
 55. Thottappillil, R., M.A. Uman, and V.A. Rakov, *Treatment of retardation effects in calculating the radiated electromagnetic fields from the lightning discharge*. *Journal of Geophysical Research*, 1998. **103**(D8): p. 9003-13.
 56. Cooray, V., et al. *On the constraints imposed by the close electric field signature on the equivalent corona current in lightning return stroke models*. in *International Conference on Lightning Protection (ICLP 2004)*. 2004. Avignon, France.
 57. Pavanello, D., et al. *Propagation effects on the electromagnetic field radiated by lightning to tall towers*. in *VIII International Symposium on Lightning Protection, SIPDA*. 2005. Sao Paulo, Brazil.
 58. Cooray, V., *Effects of propagation on the return stroke radiation fields*. *Radio Science*, 1987. **22**(5): p. 757-68.
 59. Pavanello, D., et al. *Electromagnetic environment in the immediate vicinity of a tower struck by lightning*. in *EUROEM'2004*. 2004. Magdeburg, Germany.
 60. Miyazaki, S. and M. Ishii. *Influence of elevated stricken object on lightning return-stroke current and associated fields*. in *International Conference on Lightning Protection ICLP*. 2004. Avignon, France.